RECENT LEP2 RESULTS ON SEARCHES FOR NEW PHENOMENA

Yibin Pan*
Department of Physics, University of Wisconsin
1150 University Ave., Madison, WI 53706, USA

ABSTRACT

Recent results of searches for supersymmetric particles, Higgs bosons, and other new phenomena at LEP2 are summarized. These results are based on data and analyses from the four LEP experiments: ALEPH, DELPHI, L3, and OPAL. The data were collected during the summer and fall of 1996 with center-of-mass energies of 161 and 172 GeV.

*Supported by DOE Contract DE-FG0295-ER40896.

1 Introduction

One of the major objectives of the LEP program is the search for new phenomena beyond the current results of high-energy physics experiments. In the summer of 1996, LEP was upgraded (LEP2), and for the first time, a center-of-mass energy above the threshold for the production of W pairs was achieved. The higher center-of-mass energy provides a great opportunity to search for new phenomena.

In 1996, two sets of data were collected by each of the four LEP experiments: one at a center-of-mass energy of 161 GeV, and the other at 172 GeV. An integrated luminosity of about 10 to 11 pb^{-1} per experiment was collected at each of these two energy points. The results presented in this review are based on these 1996 LEP2 data.*

This review summarizes recent results of searches performed by the four LEP experiments; it includes searches for supersymmetric particles and Higgs bosons, as well as searches for anomalous production of four-jet final states.

2 Searches for Supersymmetric Particles

The searches discussed in this section are mostly in the context of the Minimal Supersymmetric Standard Model (MSSM). MSSM predicts supersymmetric (SUSY) partners for each of the particles in the Standard Model (SM). These SUSY particles include:

- Sleptons ($\tilde{\mathrm{e}}$, $\tilde{\mu}$, $\tilde{\tau}$, $\tilde{\nu}$): the SUSY partners of the SM charged and neutral leptons;
- Charginos ($\tilde{\chi}_1^{\pm}$, $\tilde{\chi}_2^{\pm}$): the mass eigenstates from the SUSY partners of $\mathrm{H}^{\pm}$† and $\mathrm{W}^{\pm}$;
- Neutralinos ($\tilde{\chi}_1^0$, $\tilde{\chi}_2^0$, $\tilde{\chi}_3^0$, $\tilde{\chi}_4^0$): the mass eigenstates from the SUSY partners of H_1^0, H_2^0, γ, and Z;

*At the time of writing, LEP had finished its 1997 data collecting program. In 1997, each LEP experiment collected about 60 pb^{-1} at a center-of-mass energy of 183 GeV plus about 3 pb^{-1} at both 130 and 136 GeV. To bring this review more up-to-date, some results based on preliminary analyses of these 1997 data are shown or mentioned in various places in the text, but it should be noted that these results are neither final nor "official."

†In the MSSM, the Higgs spectrum contains two CP-even and one CP-odd neutral Higgs bosons, (H, h) and A, respectively, in addition to a charged Higgs boson pair $\mathrm{H}^{\pm}$.

- Squarks ($\tilde{\mathrm{t}}$, $\tilde{\mathrm{b}}$, etc.): the SUSY partners of the quarks;
- Gluinos ($\tilde{\mathrm{g}}$): the SUSY partners of the gluons.

For the chargino and neutralino searches, only the lighter candidates ($\tilde{\chi}^{\pm}_1$, $\tilde{\chi}^0_1$, $\tilde{\chi}^0_2$) are studied in detail. The squark analyses only search for $\tilde{\mathrm{t}}$ and $\tilde{\mathrm{b}}$, which are believed to be lighter than the others. Among the sleptons, the charged candidates $\tilde{\mathrm{e}}$, $\tilde{\mu}$, and $\tilde{\tau}$ are searched for ($\tilde{\nu}$ is not detectable directly in the LEP detectors).

In the MSSM, a quantum number called R-parity is defined to be -1 for SUSY particles, and $+1$ for SM particles. R-parity conservation is not required by all SUSY theories, but it is generally assumed to hold for many of the analyses including those presented in this review.‡ If R-parity conservation is assumed, then all SUSY particles must be produced in pairs and decay into, among other particles, the lightest SUSY particle (LSP). The LSP is stable and cannot decay. With the support of some cosmological arguments and other experimental evidence, the lightest neutralino ($\tilde{\chi}^0_1$) is assumed to be the LSP. Hence, while it carries away energy, the $\tilde{\chi}^0_1$ cannot be detected directly in the detector. These assumptions lead to an important signature for events involving SUSY particles, i.e., sizable missing energy in the detector.

Table 1 summarizes the processes and the event topologies involved in the SUSY particle searches. The main backgrounds here are SM processes: the radiative Z return process ($\mathrm{e^+e^-} \longrightarrow \gamma\mathrm{Z}$), W pair and Z pair production ($\mathrm{e^+e^-} \longrightarrow$ WW, ZZ), and the two-photon process ($\gamma\gamma \longrightarrow f\overline{f}$).

There is no evidence for the production of any of these SUSY particles in the LEP2 data. Several candidates for the topology described above are selected in each experiment, but they are all in agreement with predictions of SM processes.

Space restrictions preclude the presentation of all results, but the plots in Fig. 1 to Fig. 4 show some of the 95% C.L. exclusions obtained from SUSY searches. In many cases, the four LEP experiments all have similar analyses; the ones shown are only representative of these results.§ More details of the analyses and results can be found in Refs. 1, 2, and 3.

‡Analyses without the assumption of R-parity conservation have also been performed at LEP. However, the length requirements of this article preclude discussion of these searches.

§As indicated in the figures, some of the results are obtained after combining individual analyses of several LEP experiments.

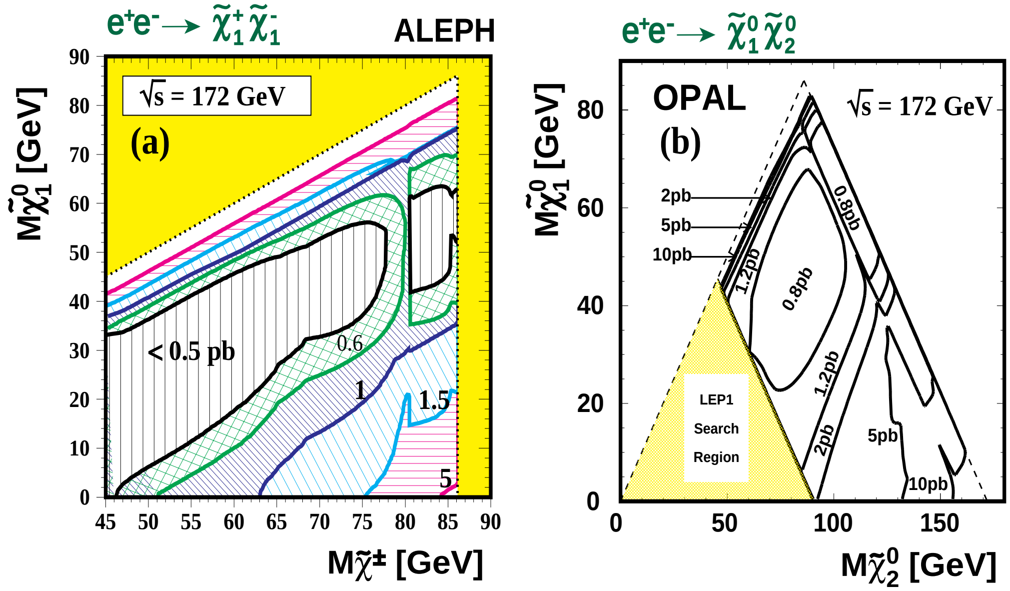

Fig. 1. Cross section limit from the (a) ALEPH $\tilde{\chi}_1^{\pm}$ searches and (b) OPAL $\tilde{\chi}_2^0$ searches. Exclusion regions in the MSSM parameter space can be deduced from these cross section limits.

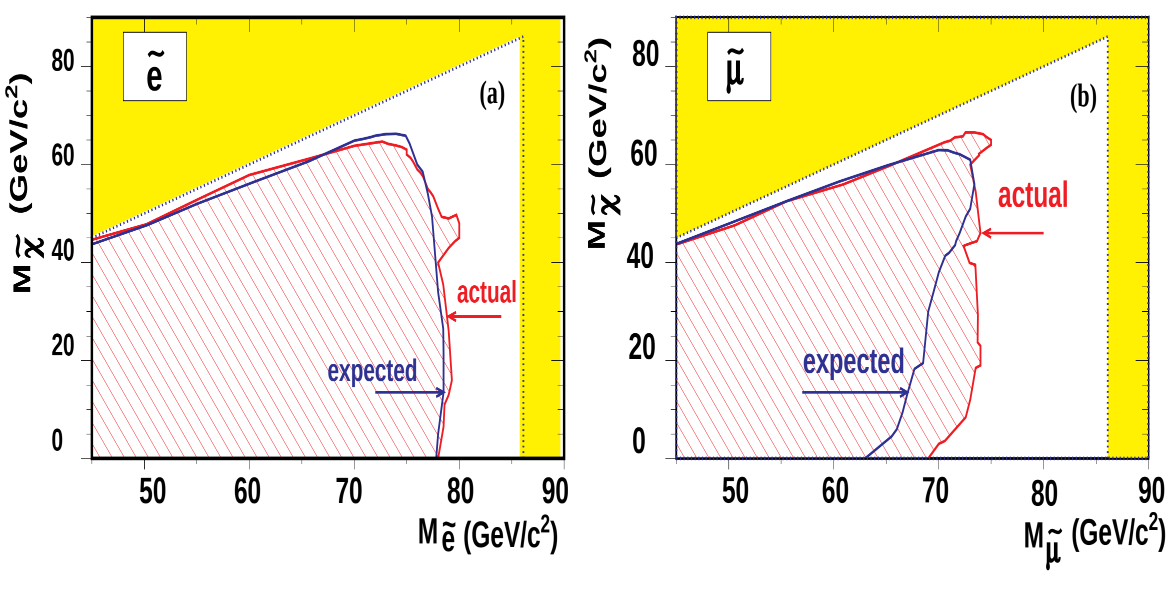

Fig. 2. Slepton mass limits as a function of the mass of the lightest neutralino. Results from all four LEP experiments are combined. The limits are at 95% C.L.

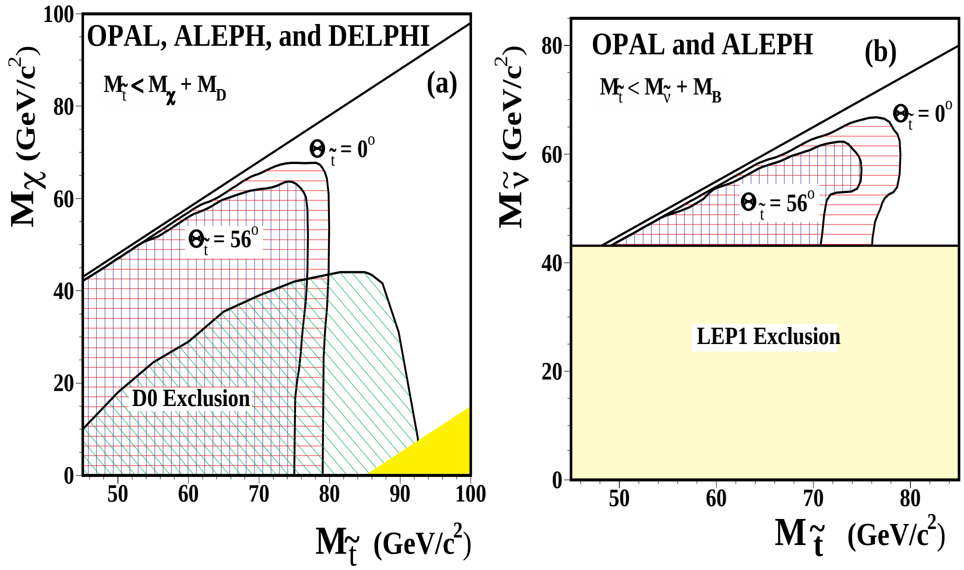

Fig. 3. 95% C.L. limits for the top squark mass. Two possible top squark decay modes are studied: (a) $\tilde{t} \longrightarrow c\tilde{\chi}_1^0$ and (b) $\tilde{t} \longrightarrow b\ell^+\tilde{\nu}$. Two assumed values of the mixing angle $\theta_{\tilde{t}}$ between the right and left states of the top squark are used in both plots.

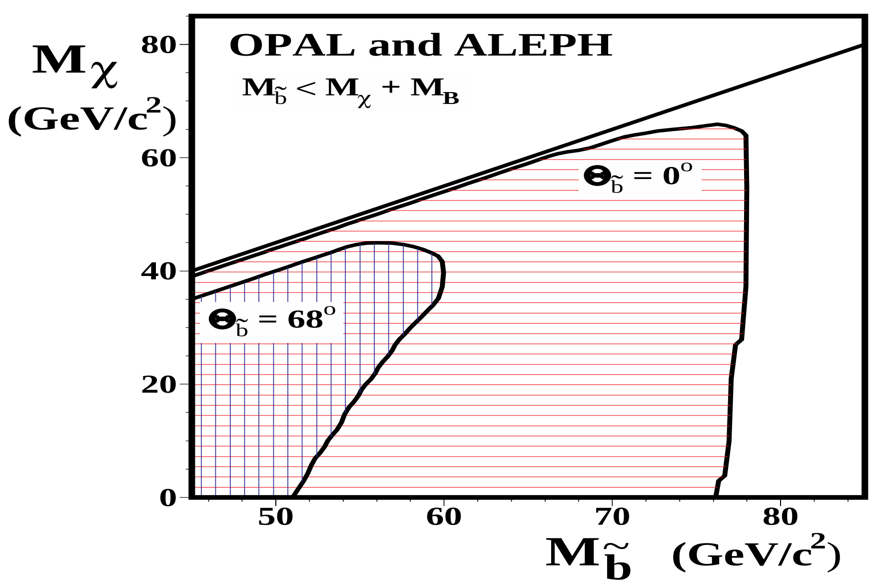

Fig. 4. 95% C.L. limit for the bottom squark mass. The bottom squark decay mode of $\tilde{b} \longrightarrow b\tilde{\chi}_1^0$ is assumed. Two assumed values of the mixing angle $\theta_{\tilde{b}}$ between the right and left states of the bottom squark are used in both plots.

Table 1. Processes in the SUSY particle searches, assuming the $\tilde{\chi}_1^0$ is the LSP. $\not{E}$ denotes the missing energy in the detector.

	Production	Decay	Topology
Charginos	$e^+e^- \longrightarrow \tilde{\chi}^+\tilde{\chi}^-$	$\tilde{\chi}^+ \longrightarrow W^*\tilde{\chi}_1^0$	jets + $\not{E}$ jets + ℓ+ $\not{E}$ $\ell^+\ell^-$ + $\not{E}$
Neutralinos	$e^+e^- \longrightarrow \tilde{\chi}_1^0\tilde{\chi}_2^0$	$\tilde{\chi}_2^0 \longrightarrow Z^*\tilde{\chi}_1^0$	jets + $\not{E}$ $\ell^+\ell^-$ + $\not{E}$
Sleptons	$e^+e^- \longrightarrow \tilde{\ell}^+\tilde{\ell}^-$	$\tilde{\ell} \longrightarrow \ell\tilde{\chi}_1^0$	$\ell^+\ell^-$ + $\not{E}$
Top Squark	$e^+e^- \longrightarrow \tilde{t}\bar{\tilde{t}}$	$\tilde{t} \longrightarrow c\tilde{\chi}_1^0$ or $\tilde{t} \longrightarrow b\ell^+\tilde{\nu}$	jets + $\not{E}$ jets + $\ell^+\ell^-$ + $\not{E}$

Table 2. Lower mass limits on the lightest neutralino.

ALEPH	DELPHI	L3	OPAL
25 GeV	24.9 GeV	24.6 GeV	24.7 GeV

One of these results has special interest for cosmological studies, the mass limit on the lightest neutralinos. The Lightest Supersymmetric Particle (LSP) is a good candidate for the dark matter of the universe, and the lightest neutralino is thought most likely to be the LSP. Therefore, a limit on its mass is relevant. Assuming gauge unification in the MSSM, this limit can be obtained by combining the results of the searches for $\tilde{\chi}_1^\pm$ and $\tilde{\chi}_2^0$. Table 2 lists the lower limits on the $\tilde{\chi}_1^0$ from the four LEP experiments. The limits are at 95% C.L. and are valid only when tan$\beta > 1$ and $M_{\tilde{\nu}} > 200$ GeV. For the minimum allowed $M_{\tilde{\nu}}$, the limits are lower; ALEPH and OPAL have obtained $M_{\tilde{\chi}_1^0} > 14$ and 13.3 GeV, respectively. Preliminary results show that if the 1997 183 GeV data are included, these limits will increase by about 5 GeV.

3 Search for the Standard Model Higgs Boson

The Higgs boson H^0 is a key element in the Standard Model. At LEP2 energies, the Higgs boson H^0 can be produced via the Higgs-strahlung process or WW and ZZ processes, as shown in Fig. 5(a). The fusion processes are typically an order of magnitude smaller than the strahlung process. So the Higgs boson is searched for only via the strahlung process at LEP2. Figure 5(b) gives the production cross sections as a function of the Higgs boson mass at LEP1 and LEP2 energies. The decay modes and event topology are shown in Table 3.

Table 3. Decay modes and event topology of the Higgs-strahlung process.

Production Channel	Decay Modes	Topology
$e^+e^- \longrightarrow H^0Z$	$H \longrightarrow b\overline{b},\ \tau^+\tau^-,\ c\overline{c}$ $Z \longrightarrow q\overline{q},\ \nu\overline{\nu},\ \ell^+\ell^-$	$b\overline{b}q\overline{q},\ b\overline{b}\ell\overline{\ell},\ b\overline{b}\nu\overline{\nu},\ \tau\overline{\tau}q\overline{q}$

Given the fact that neutral Higgs bosons decay predominantly to two b jets,¶ all four experiments have used effective b-tagging algorithms in the analyses. b jets are identified mainly by exploiting the longer lifetime and higher mass of b hadrons compared to other hadrons, but also by the presence in the jets of high-p_T leptons from semileptonic decays. To use the lifetime information in a given jet, track impact parameters and secondary decay vertices are reconstructed relative to an event-by-event interaction point. As an example, in ALEPH six variables which discriminate between b jets and light quark jets are combined using neural networks to tag b quark jets. The first two variables are lifetime-based; the third is based on the transverse momentum of identified leptons and the last three are based on jet-shape properties. Figure 6 shows the output η of the neural network b tag for radiative returns to the Z for the 161 GeV $q\bar{q}$ Monte Carlo (histogram) compared to the data at 161 GeV (points). The shaded region shows the contribution from generated b jets. Figure 7 shows the performance of the neural network b tag (solid line) for Monte Carlo events, presented in terms of the efficiency for identifying b jets versus the efficiency for rejecting light quark jets. The performance of the single most powerful b-tagging input variable to the neural network

¶At the mass range we are interested in, the b decay branching ratios are about 85% for H^0.

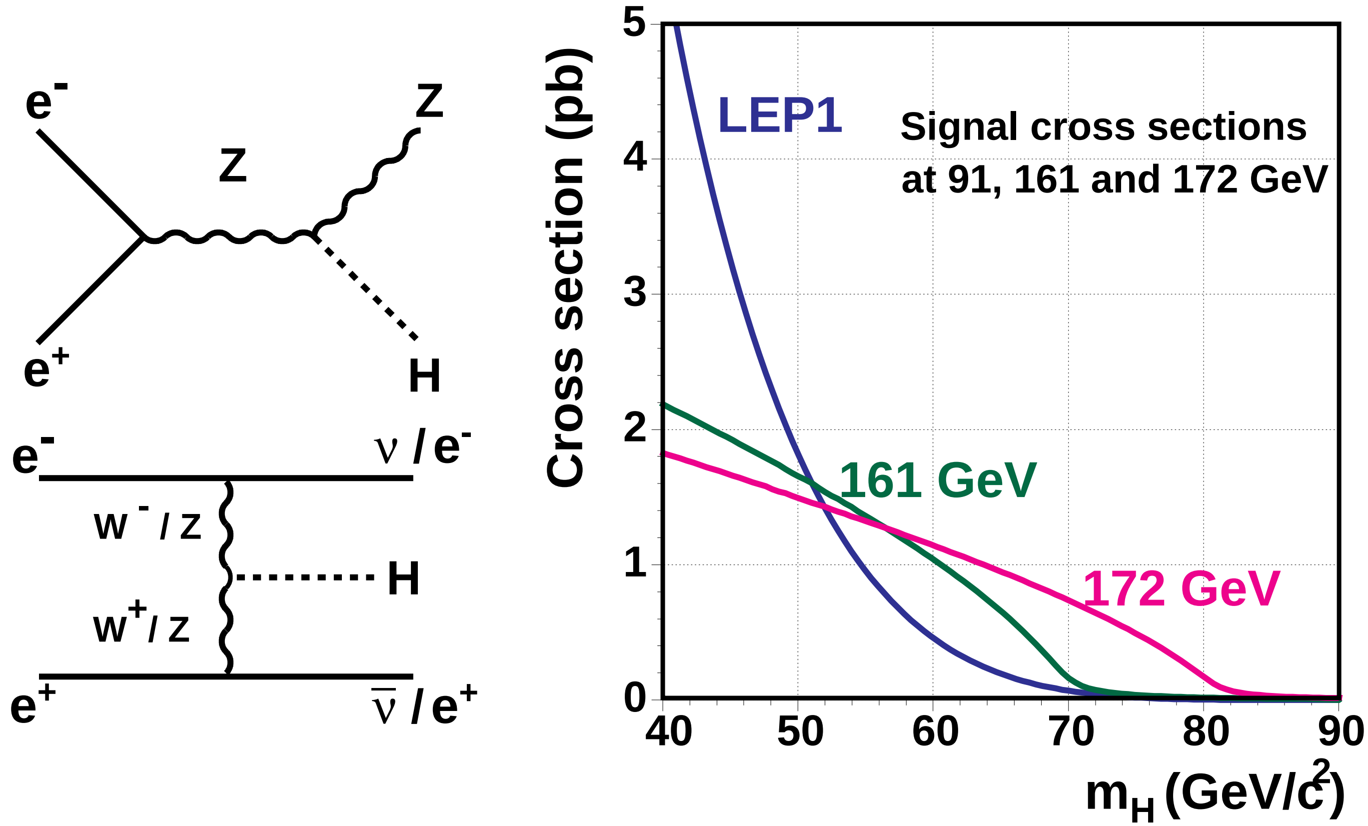

Fig. 5. (a) Feynman diagrams for the Higgs-strahlung process (top) and for the WW or ZZ fusion process (bottom). (b) The corresponding production cross sections as a function of the Higgs boson mass at LEP1 energies, at 161 GeV, and at 172 GeV.

is shown for comparison (dashed curve). Figure 8 shows the separation power in Monte Carlo of the neural network outputs of the two most b-like jets (NN_3 and NN_4) in (a) HZ signal, (b) qqg background, and (c) WW background in the HZ $\rightarrow b\overline{b}q\overline{q}$ channel.

No evidence of the SM Higgs boson H^0 has been observed in the 1996 LEP2 data. The lower mass limits provided in Table 4 are obtained from the analyses described in Ref. 4. Figure 9 shows the ALEPH results on the lower limit for the SM neutral Higgs boson. In addition, preliminary analysis shows that if the results of the four LEP experiments are combined, the lower mass limit can be set at 77.5 GeV for the SM Higgs, as shown in Fig. 10.

Table 4. Lower mass limits (in GeV) at 95% C.L. for Higgs bosons.

	ALEPH	DELPHI	L3	OPAL
$M_{H^0} >$	70.7	66.2	69.5	69.4

4 Searches for Higgs Bosons Beyond the SM

In minimal extensions of the SM, two Higgs doublets are introduced in order to give masses to up-type quarks and down-type quarks separately. In these models, the Higgs sector therefore consists of five physical states, namely three neutral bosons—two CP-even h and H, and one CP-odd A—and a pair of charged bosons $H^{\pm}$. Six independent parameters are required: four Higgs boson masses, the ratio $v_1/v_2 \equiv \tan\beta$ of the vacuum expectation values of the two Higgs doublets, and α, the mixing angle in the CP-even sector.

Predictions can therefore only be made in specific models, of which the most popular is the Minimal Supersymmetric extension of the Standard Model (MSSM). In this model, both H and $H^{\pm}$ are predicted to be too heavy to be discovered at LEP2. The analysis presented here is consequently restricted to the search for the lighter Higgs bosons, h and A, which can be produced by two complementary processes, the Higgs-strahlung process $e^+e^- \longrightarrow hZ$ with a cross section proportional to $\sin^2(\beta-\alpha)$ and the associated pair-production $e^+e^- \longrightarrow hA$ with a cross section proportional to $\cos^2(\beta-\alpha)$, as shown in Fig. 11. The decay modes and event topology of these two processes are shown in Table 5.

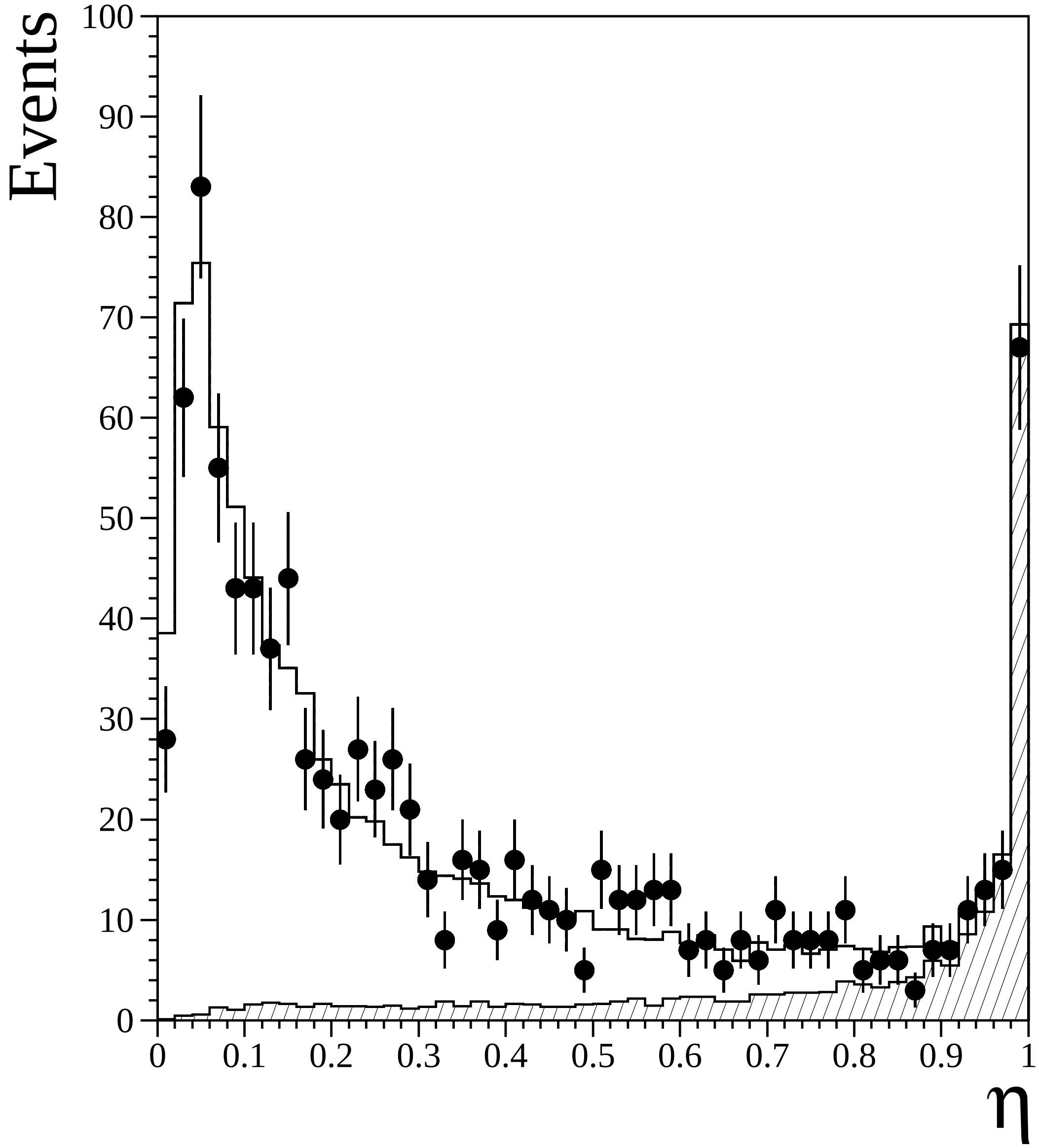

Fig. 6. The output η of the neural network b tag for radiative returns to the Z for the 161 GeV $q\bar{q}$ Monte Carlo (histogram) compared to the data at 161 GeV (points). The shaded region shows the contribution from generated b jets.

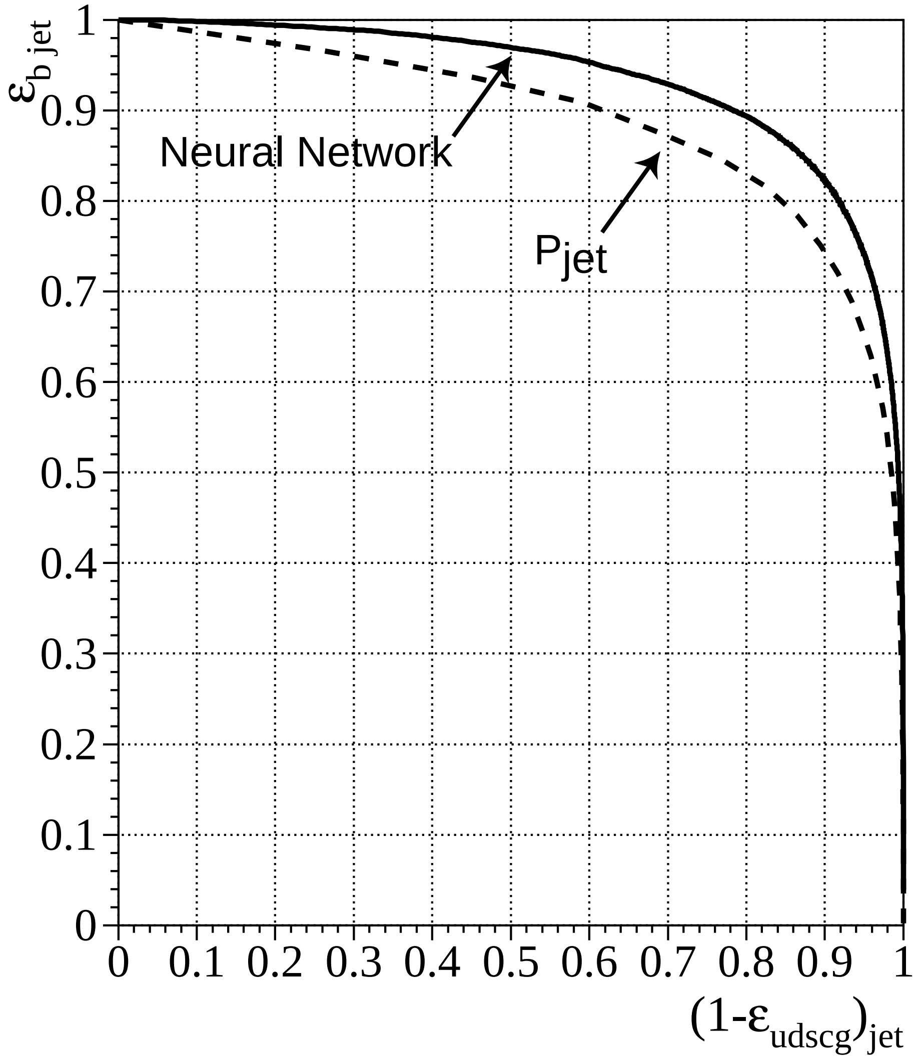

Fig. 7. The performance of the neural network b tag (solid line) for Monte Carlo events, presented in terms of the efficiency for identifying b-jets vs the efficiency for rejecting light quark jets. The performance of the single most powerful b-tagging input variable to the neural network is shown for comparison (dashed curve).

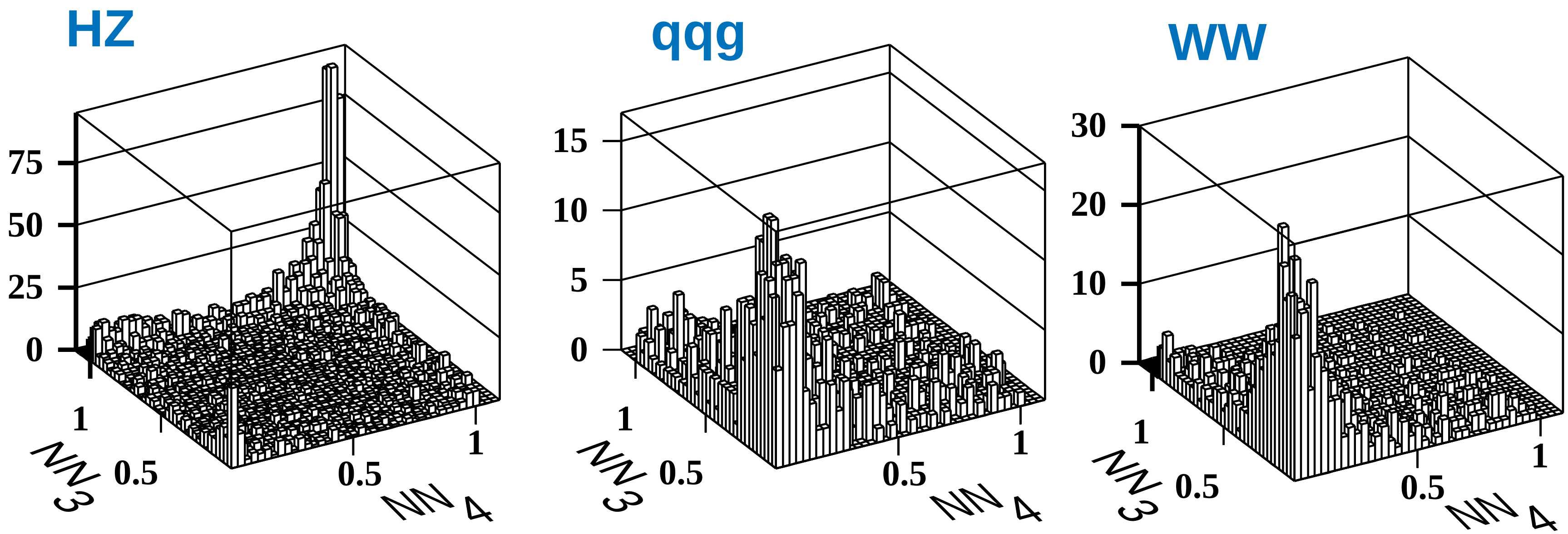

Fig. 8. The separation power in Monte Carlo of the neural network outputs of the two most b-like jets (NN_3 and NN_4) in the (a) HZ signal, (b) qqg background, and (c) WW background in the $HZ \rightarrow b\bar{b}q\bar{q}$ channel.

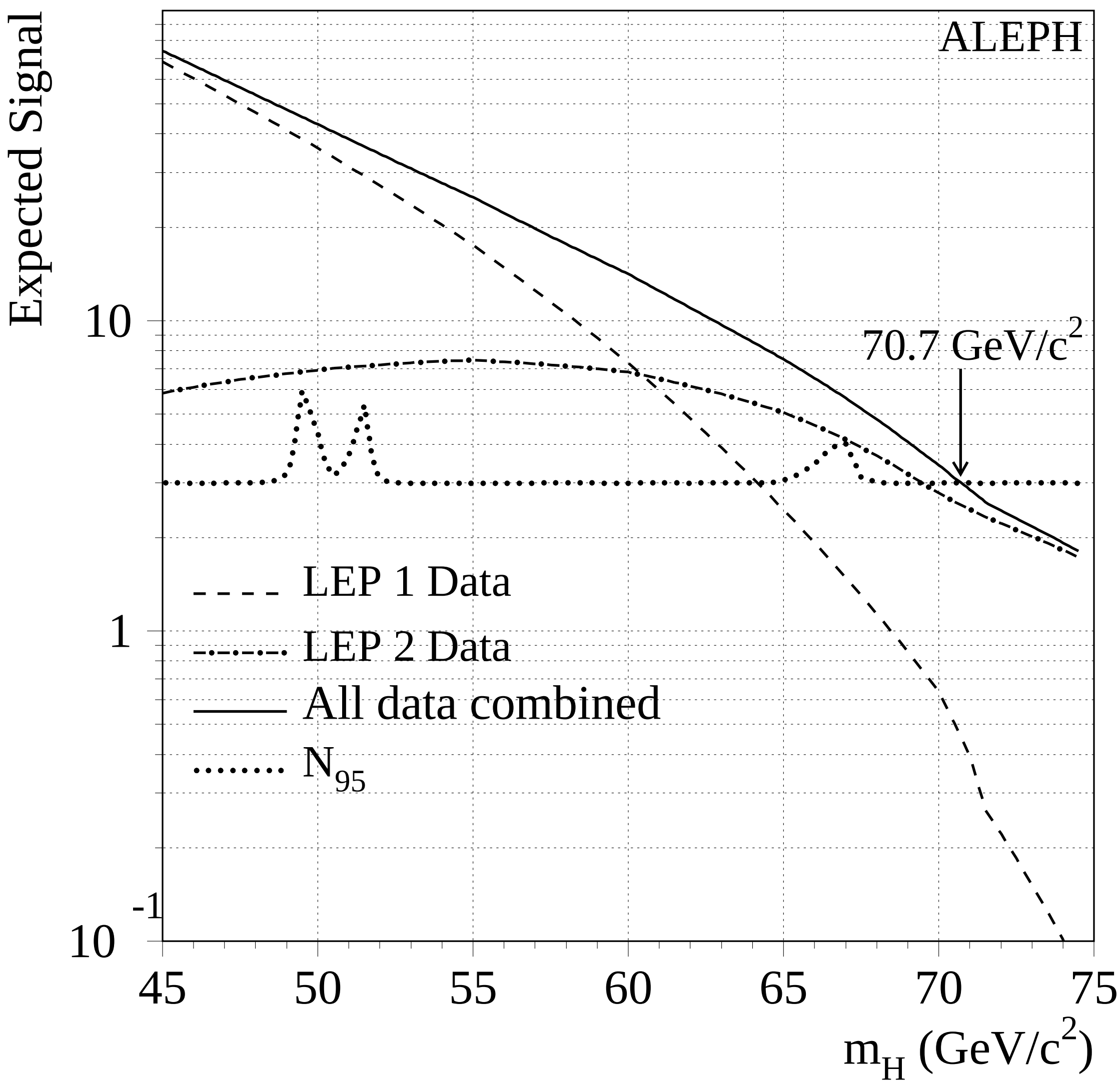

Fig. 9. Number of events expected for signal from high-energy data (dashed dotted curve), the LEP1 data (dashed curve), and the combination (full curve). The dotted curve indicates the number of signal events needed to reach a confidence level of 5%. The bumps are due to the three candidate events found at LEP1 in the $H\mu^+\mu^-$ channel.

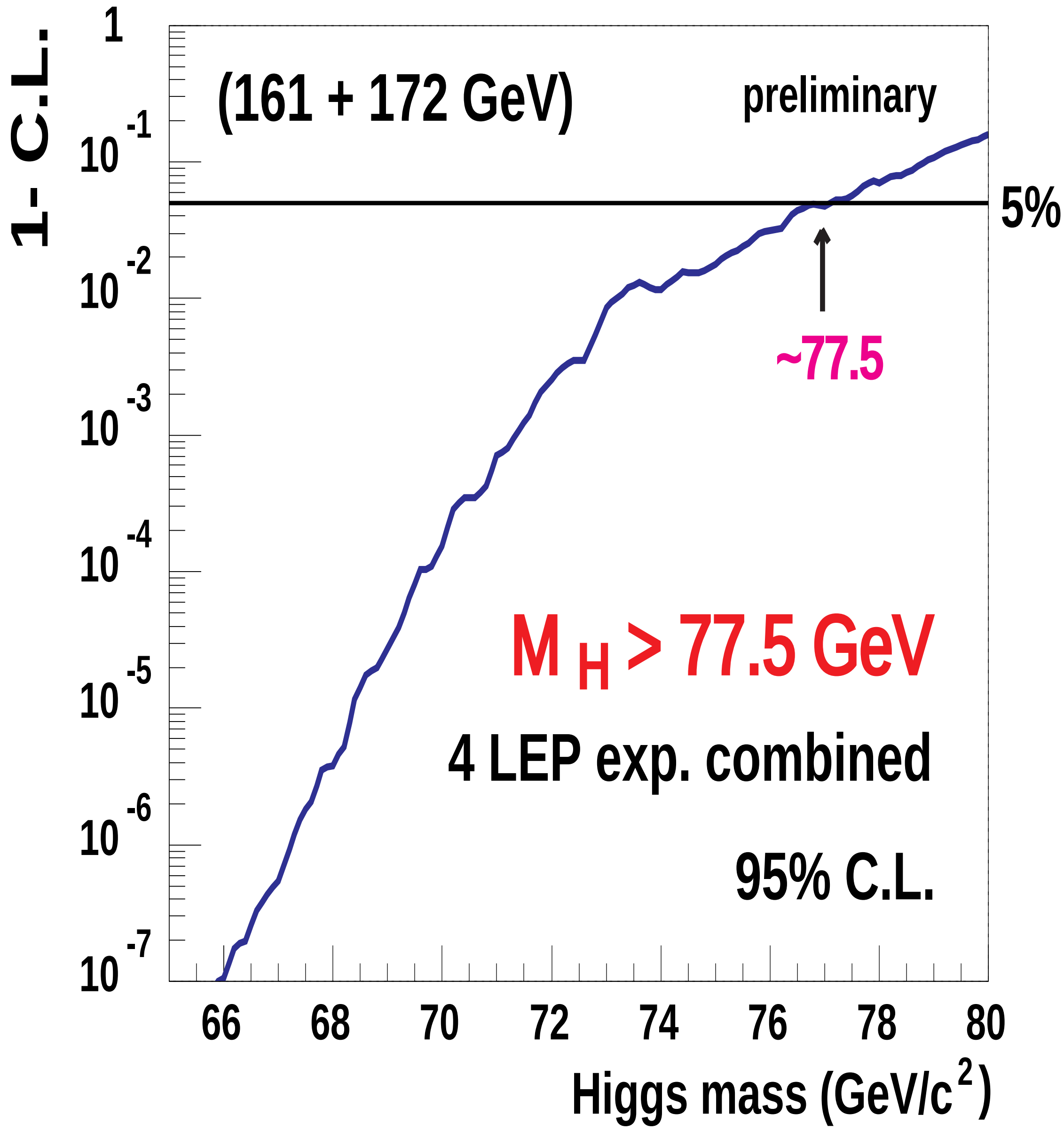

Fig. 10. The combined confidence level curve of the four LEP experiments (preliminary).

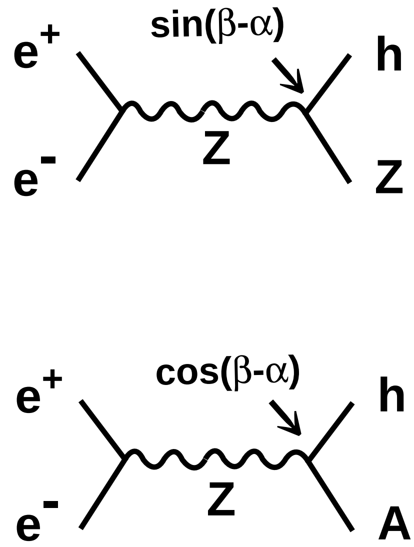

Fig. 11. Feynman diagrams for $e^+e^- \longrightarrow hZ$ (top) and $e^+e^- \longrightarrow hA$ (bottom).

Table 5. Processes involved in the searches for neutral Higgs bosons in the MSSM.

Production Channel	Decay Modes	Topology
$e^+e^- \longrightarrow hZ$	$H \longrightarrow b\bar{b}$, $\tau^+\tau^-$ $Z \longrightarrow q\bar{q}$, $\nu\bar{\nu}$, $\ell^+\ell^-$	$b\bar{b}q\bar{q}$, $b\bar{b}\ell\bar{\ell}$, $b\bar{b}\nu\bar{\nu}$, $\tau\bar{\tau}q\bar{q}$
$e^+e^- \longrightarrow hA$	$h \longrightarrow b\bar{b}$, $\tau^+\tau^-$ $A \longrightarrow b\bar{b}$, $\tau^+\tau^-$	$b\bar{b}b\bar{b}$, $\tau\bar{\tau}b\bar{b}$

At tree-level, only two parameters are needed to determine all the other relevant quantities (masses, couplings, and therefore, cross sections). Here, these are chosen to be $\tan\beta$ and the mass m_h. For $m_h = 60$ GeV/c^2 and $\tan\beta = 10$, the branching fraction of h and A to $b\bar{b}$ is 92% and to $\tau^+\tau^-$ is 8%, giving $b\bar{b}b\bar{b}$ final states in 84% of the events and $\tau^+\tau^- b\bar{b}$ in 14%. Analyses of both these channels are performed.

No significant excess of events from the search for the process of $e^+e^- \longrightarrow hA$ were observed. The results are combined with the results of the search for the Higgs-strahlung process $e^+e^- \longrightarrow hZ$. Table 6 gives the limits on m_h for the four

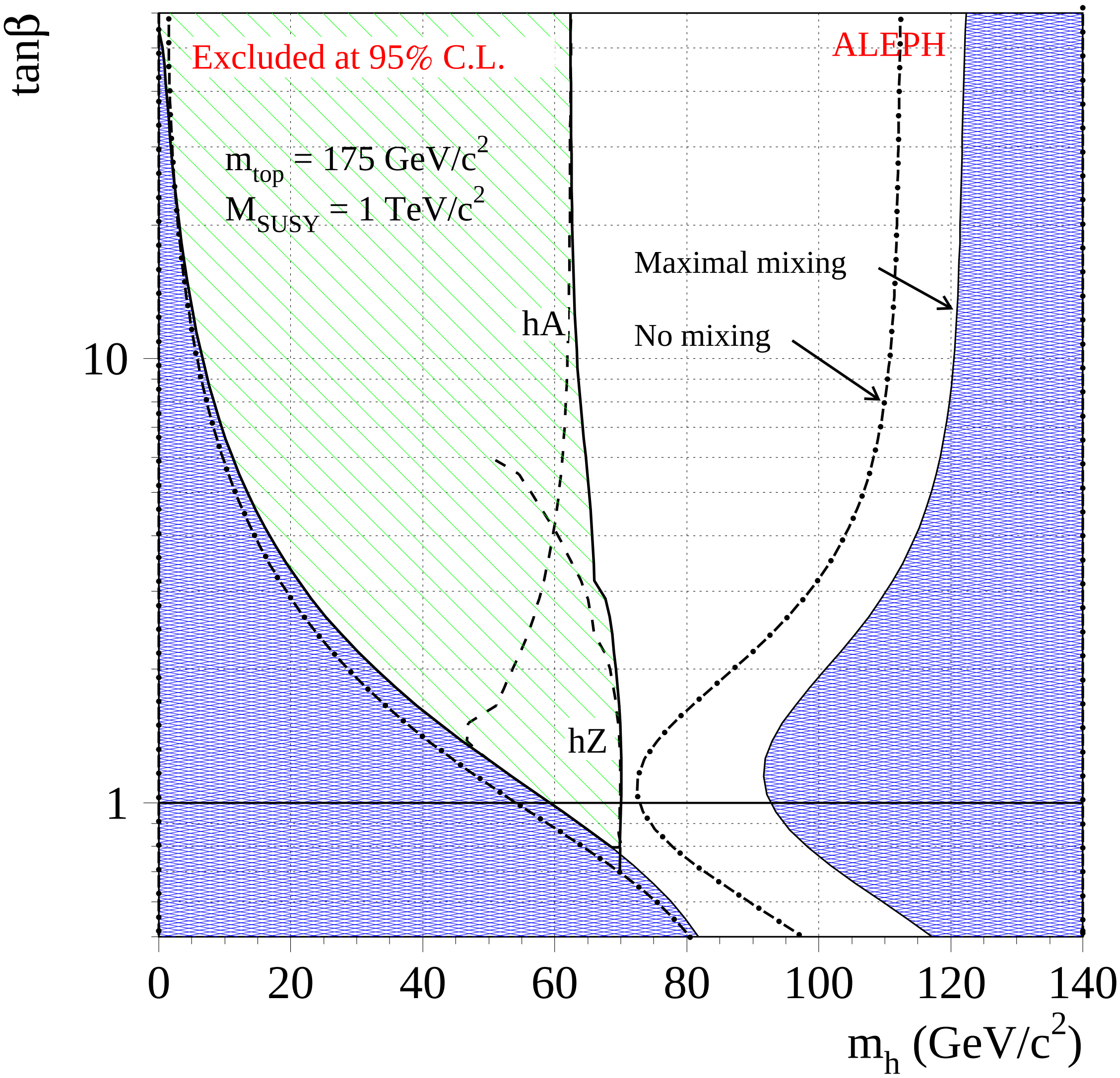

Fig. 12. ALEPH results on the $[m_h, \tan\beta]$ plane in the configuration with maximal mixing between the right and left states of the top squark. The dark area is theoretically disallowed. The hatched area is excluded at the 95% confidence level by the combined search for $e^+e^- \longrightarrow hA$ and $e^+e^- \longrightarrow hZ$. The dot-dashed lines show the change in the theoretical region in the no-mixing configuration.

LEP experiments.[5] The highest individual limit was at 62.5 GeV/c^2. Figure 12 gives the 95% C.L. excluded region in the $[m_h, \tan\beta]$ plane for ALEPH.

Table 6. Lower mass limits (in GeV/c^2) at 95% C.L. for neutral Higgs bosons in the MSSM.

	ALEPH	DELPHI	L3	OPAL
m_h $>$	62.5	59.5	58.4	56.1

For the more general models containing two Higgs doublets, the MSSM constraints do not exist. Figures 13 and 14 show the DELPHI results[6] for the excluded regions for CP-conserving and non-CP-conserving scenarios respectively.

Charged Higgs pair production has also been searched for at LEP.[7] The analyses are performed in a model-independent way. Only two decay modes of $H^{\pm}$, $\tau\bar{\nu}$ and $c\bar{s}$, are assumed. As a result, in each experiment three analyses are employed to select the $\tau^{+}\nu_{\tau}\tau^{-}\bar{\nu_{\tau}}$, $c\bar{s}\tau^{-}\bar{\nu}_{\tau}$, and $c\bar{s}\bar{c}s$ final states. No evidence for a signal is found. In Fig. 15, mass limits are set as a function of the branching fraction Br($\tau\nu$) for $H^{\pm} \to \tau\nu$ for OPAL. Table 7 gives lower mass limits at 95% C.L. for the four LEP experiments.

Table 7. Lower mass limits (in GeV/c^2) at 95% C.L. for charged Higgs bosons.

	ALEPH	DELPHI	L3	OPAL
$m_{H^{\pm}}$ $>$	52.0	54.5		52.0

In the SM, the decay modes H $\to$ invisible and H $\to \gamma\gamma$ are predicted to be rare. But in some nonminimal extensions to the SM, these decay modes can be greatly enhanced or even be dominant. In the production of $e^{+}e^{-} \to$ hZ, the decay channels considered involve both hadronic and leptonic final states for the Z boson, and invisible or di-photon final states for the Higgs boson. Figure 16 shows the limit on the Higgs mass as a function of the H $\to$ invisible decay branching ratio obtained by L3 (Ref. 8). ALEPH has a similar result. Figure 17 gives the limit obtained by OPAL[9] on Br(H $\to \gamma\gamma$).

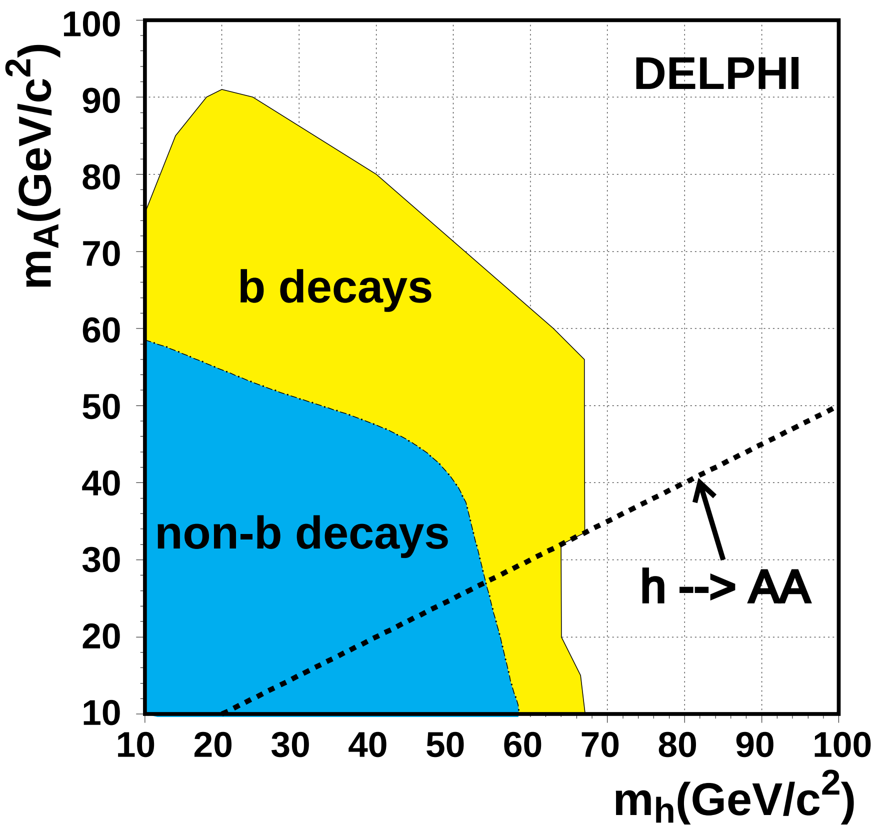

Fig. 13. DELPHI results for excluded regions at the 95% C.L. in the CP-conserving model, assuming b decays are dominant (light gray), and allowing for non-b decays (dark gray).

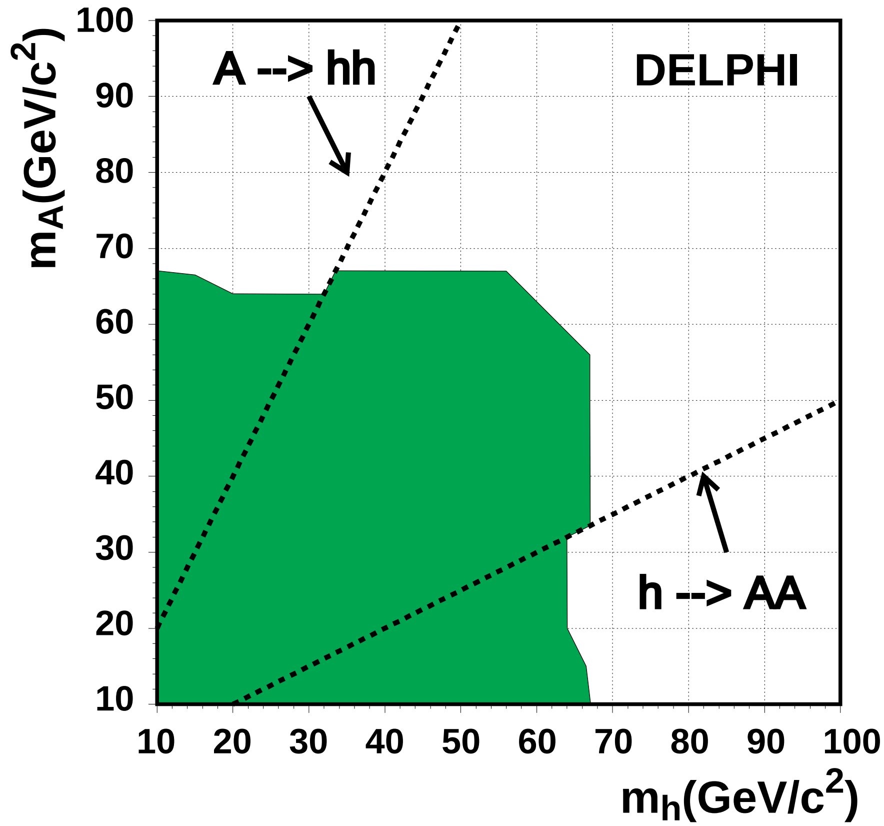

Fig. 14. DELPHI results for excluded regions at the 95% C.L. in the non-CP-conserving model.

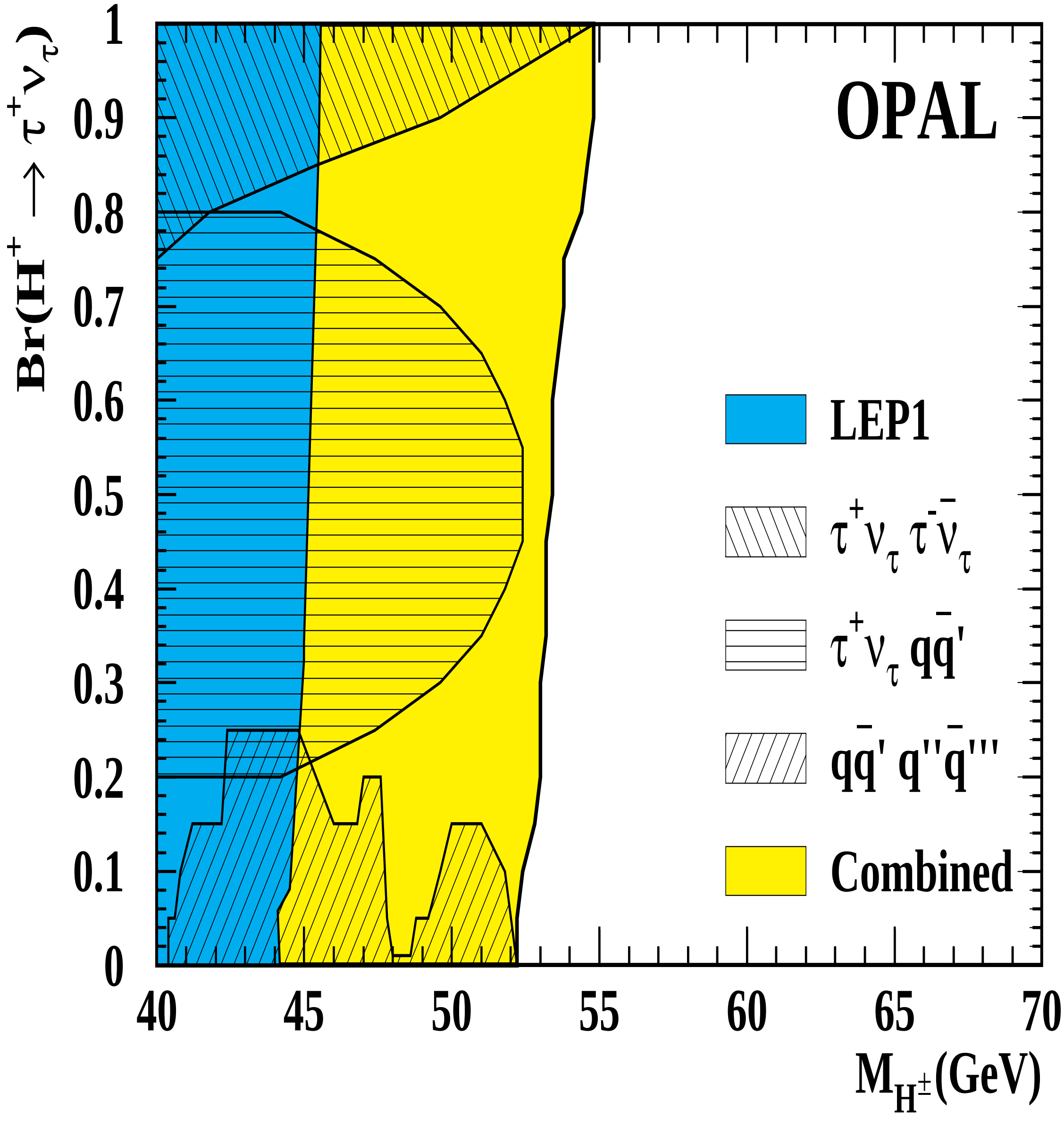

Fig. 15. OPAL limits at 95% C.L. on the mass of charged Higgs bosons as a function of Br($\tau\nu$).

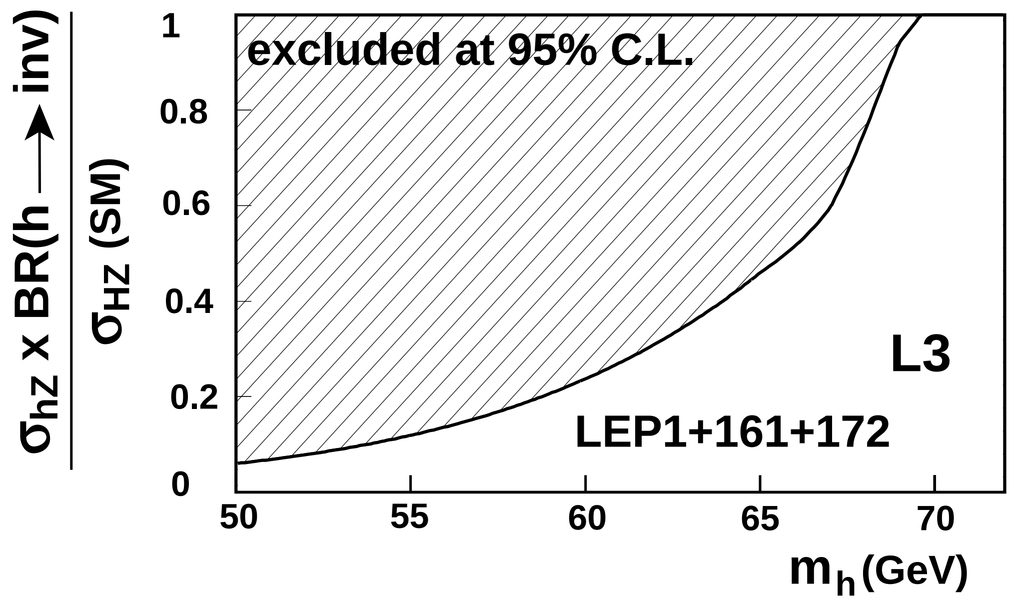

Fig. 16. Upper limits on the rate of invisible Higgs decays, relative to the SM Higgs production rate, by L3.

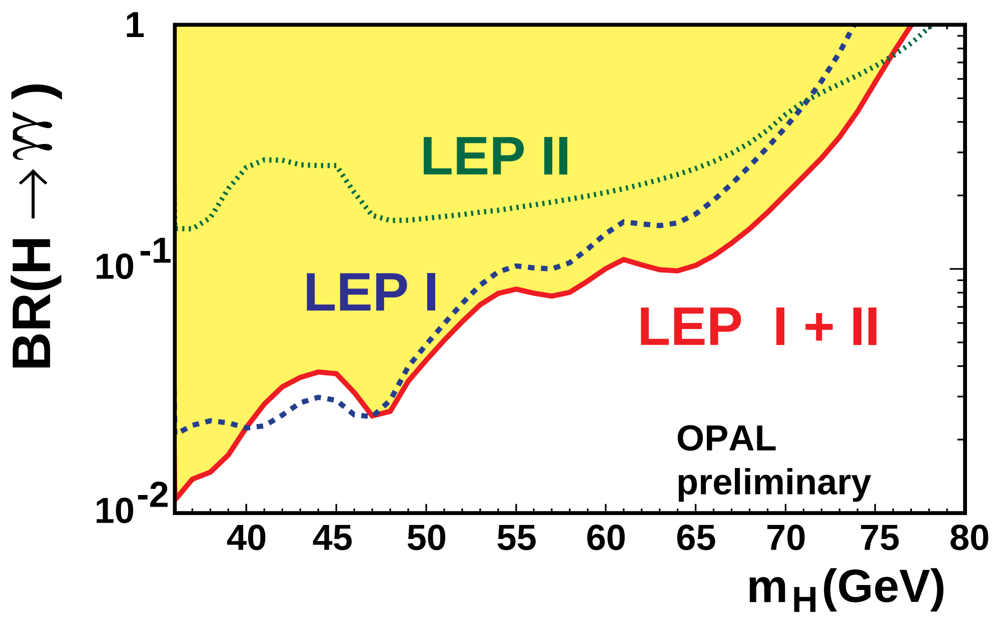

Fig. 17. OPAL 95% C.L. upper limit on Br(H $\rightarrow \gamma\gamma$) for SM Higgs boson production using data from LEP1 (dashed line), LEP2 (dotted line), and all data combined (solid line).

5 Searches for Anomalous Four-Jet Production

Searches in four-jet final states are inspired by an earlier analysis[10] performed by the ALEPH Collaboration with the 1995 LEP data collected at center-of-mass energies of 130 and 136 GeV. Events kinematically similar to the $e^+e^- \longrightarrow hA \longrightarrow$ 4-jet-type topology were selected, and the sum of the di-jet masses (analogous to $M_h + M_A$) was calculated for each selected event. Sixteen events were selected. Nine events had di-jet mass sums clustering around 105 GeV. The SM predicts only 8.6 events and a flat spectrum for the mass sum. No b enhancement was found in these events. Following ALEPH, the other three experiments have developed analyses with similar efficiencies and mass resolution, but none of them have observed the excess or mass peak seen by ALEPH in the 130 and 136 GeV LEP data.

All four experiments have applied their analyses to the 161 GeV and 172 GeV data. While ALEPH continues to see a mass peak at 105 GeV in the new data,[‖] none of the other three experiments observe any excess in such mass spectra (see Fig. 18).

The 130 and 136 GeV data collected in 1997 provide a good opportunity to probe directly the source of this four-jet phenomenon. About 6 pb^{-1} of data, 3 pb^{-1} at 130 GeV and 3 pb^{-1} at 136 GeV, were collected by each of the LEP experiments. Analyzed in the same way as the 1995 data, the new data show no excess or mass peak in the same four-jet channel (see Fig. 19). It can be concluded that "the four-jet anomaly" ALEPH observed in their 1995 data was most likely the result of statistical fluctuation.[11]

6 Conclusion

The new data from the 1996 LEP2 runs give no evidence of new physics such as the existence of SUSY particles or Higgs bosons. However, higher center-of-mass energies at LEP2 help to extend our knowledge on particle masses and parameter spaces defined in these new physics models.

‖The total number of events selected by ALEPH from the new data is in good agreement with SM predictions.

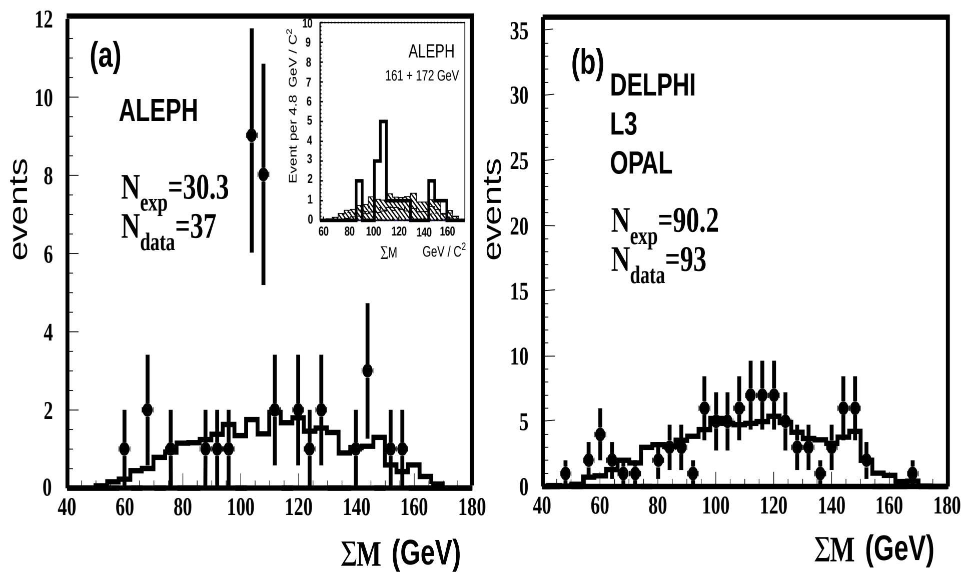

Fig. 18. Di-jet mass sum distributions for (a) ALEPH and (b) DELPHI, L3, and OPAL combined. The dots in the main figures (a) and (b) are for LEP 130-172 GeV data, and the histograms are the expectations from SM processes. The inset in (a) is for the ALEPH 161+172 GeV data only, where the SM expectation and the data are represented by hatched and unhatched histograms, respectively.

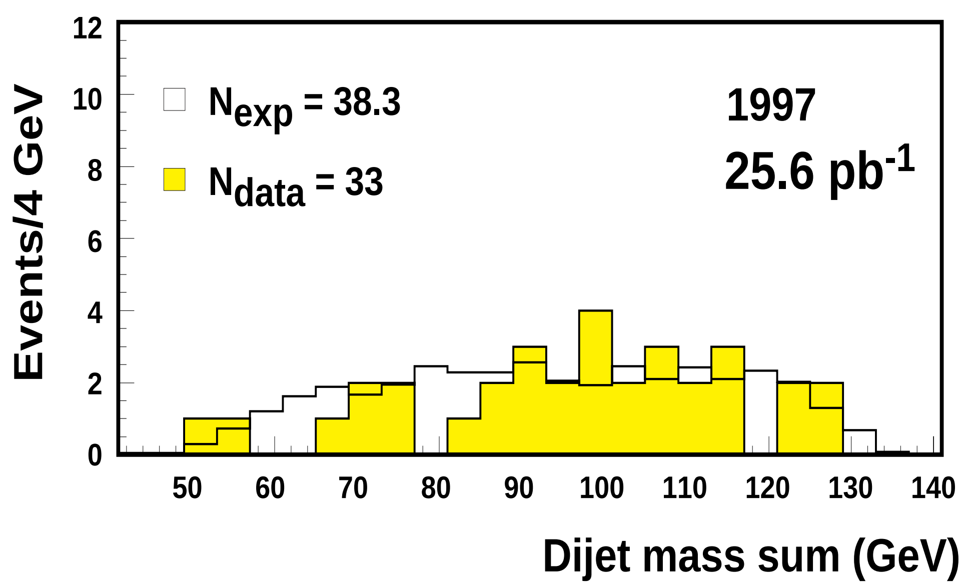

Fig. 19. Di-jet mass sum distributions for the 1997 LEP 130–136 GeV data. Results of all four LEP experiments are included in the plots.

Acknowledgments

The results presented in this review are due to the devoted work of many physicists at LEP. Many have offered me helpful information and discussions. I am grateful to all of them. The Wisconsin group at CERN and all its members provided me with great help in all aspects of my work.

This work is supported by the United States Department of Energy through grant DE-FG0295-ER40896.

References

[1] Presentations on the physics results for the LEP 161 GeV data, given at the CERN LEPC seminar on 8 October, 1996. (Ramon Miquel for ALEPH; Wim de Boer for DELPHI; Martin Pohl for L3; Nigel Watson for OPAL.)

[2] Presentations on the physics results for the LEP 172 GeV data, given at the CERN PPE seminar on 25 February, 1997. (Glen Cowan for ALEPH; Francois Richard for DELPHI; Marco Pieri for L3; Sachio Komamiya for OPAL.)

[3] The ALEPH Collaboration, R. Barate *et al.,* Phys. Lett. B **407**, 377 (1997);
The ALEPH Collaboration, R. Barate *et al.,* Phys. Lett. B **413**, 431 (1997);
The ALEPH Collaboration, R. Barate *et al.,* Phys. Lett. B **420**, 127 (1998);
The ALEPH Collaboration, R. Barate *et al.,* Eur. Phys. J. C **2**, 417 (1998);
The DELPHI Collaboration, P. Abreu *et al.,* Eur. Phys. J. C **1**, 1 (1998);
The L3 Collaboration, M. Acciarri *et al.,* Phys. Lett. B **412**, 189 (1997);
The L3 Collaboration, M. Acciarri *et al.,* Phys. Lett. B **414**, 373 (1997);
The L3 Collaboration, M. Acciarri *et al.,* Eur. Phys. J. C **4**, 207 (1998);
The OPAL Collaboration, K. Ackerstaff *et al.,* Phys. Lett. B **389**, 197 (1996);
The OPAL Collaboration, K. Ackerstaff *et al.,* Phys. Lett. B **389**, 616 (1996);
The OPAL Collaboration, K. Ackerstaff *et al.,* Zeit. für Physik C **75**, 409 (1997);
The OPAL Collaboration, K. Ackerstaff *et al.,* Phys. Lett. B **396**, 301 (1997);
The OPAL Collaboration, K. Ackerstaff *et al.,* Eur. Phys. J. C **2**, 213 (1998).

[4] The ALEPH Collaboration, R. Barate *et al.,* Phys. Lett. B **412**, 155 (1997);
The DELPHI Collaboration, P. Abreu *et al.,* Eur. Phys. J. C **2**, 1 (1998);
The L3 Collaboration, M. Acciarri *et al.,* Phys. Lett. B **411**, 373 (1997);
The OPAL Collaboration, K. Ackerstaff *et al.,* Eur. Phys. J. C **1**, 425 (1998).

[5] The ALEPH Collaboration, R. Barate *et al.,* Phys. Lett. B **412**, 173 (1997);
The DELPHI Collaboration, P. Abreu *et al.,* Eur. Phys. J. C **2**, 1 (1998);
The L3 Collaboration, M. Acciarri *et al.,* contribution to HEP'97;
The OPAL Collaboration, K. Ackerstaff *et al.,* contribution to HEP'97.

[6] The DELPHI Collaboration, P. Abreu *et al.,* contribution to HEP'97 #529.

[7] The ALEPH Collaboration, R. Barate *et al.,* Phys. Lett. B **418**, 419 (1998); The DELPHI Collaboration, P. Abreu *et al.,* Phys. Lett. B **420**, 140 (1998); The OPAL Collaboration, K. Ackerstaff *et al.,* Phys. Lett. B **426**, 180 (1998).

[8] The ALEPH Collaboration, R. Barate *et al.,* contribution to HEP'97 #617; The L3 Collaboration, M. Acciarri *et al.,* Phys. Lett. B **418**, 389 (1998).

[9] The OPAL Collaboration, K. Ackerstaff *et al.,* contribution to HEP'97 #208.

[10] The ALEPH Collaboration, D. Buskulic *et al.,* Zeit. für Physik C **71**, 179 (1996).

[11] "The Saga of the ALEPH Four Jet Events," presented by D. Schlatter at the CERN LEPC seminar on 11 November, 1997.